Density Functional Theory Study of CO Adsorption on Cu(I)-ZSM-5

Xiaobo Zheng,* Yihua Zhang, and Alexis T. Bell*

Department of Chemical Engineering, University of California, Berkeley, California 94720

Received: March 13, 2007; In Final Form: April 18, 2007

The coordination and local geometry of Cu^+ cations in Cu(I)-ZSM-5 and the adsorption of CO to such cations were explored using density functional theory. A thorough examination was made of the effects of placing Cu^+ in each of the cation-exchange sites available in the MFI lattice, the location of the Al atom in the site, and the number of Al atoms in the site. Cu^+ cations in I2 exchange sites, located at the edge of the main and sinusoidal channels, are coordinated to two framework O atoms before and after CO adsorption. The calculated adsorption energy for CO adsorbed on such cations lies between 30 and 33 kcal/mol, and the C−O vibrational frequency lies between 2150 and 2158 cm^{-1}. Cu^+ associated with five- or six-membered rings, i.e., M5, M6, Z5, and Z6 exchange sites, located in the main and sinusoidal channels of the zeolite, are 3-fold coordinated to framework O atoms, but the coordination number can decrease to 2 upon CO adsorption. The calculated CO adsorption energy of Cu^+ in such sites is in the range of 25−28 kcal/mol. Cu^+ cations located in the basket structures formed by two fused five-membered rings, in M7 sites, bind CO with a calculated adsorption energy of 21 kcal/mol. The results of this study indicate that the presence of Cu^+ cations in different exchange sites cannot be identified on the basis of infrared spectra of adsorbed CO and would be difficult to identify by temperature-programmed desorption of adsorbed CO. Evidence for two types of Cu^+ coordination can be obtained, though, from Cu K-edge extended X-ray absorption fine structure data. It is also shown that changes in Cu^+ coordination occurring upon CO adsorption can be observed by Cu K-edge X-ray absorption near-edge structure data.

Introduction

ZSM-5 zeolite exchanged with Cu^+ cations [Cu(I)-ZSM-5] is an active catalyst for a number of reactions, including NO decomposition,[1,2] the synthesis of methanol,[3] the oxidation of methanol to dimethoxymethane, and the oxidative carbonylation of methanol to dimethyl carbonate.[4] An interest has, therefore, arisen in establishing the location of the Cu^+ cations relative to the zeolite framework and the strength of interactions of the exchanged Cu^+ cations with CO, since CO is a reactant in many of the reaction systems investigated.

Several approaches have been used to introduce Cu^+ cations into the charge-exchange sites in ZSM-5. Aqueous exchange of Na-ZSM-5 (or H-ZSM-5) with a solution of $CuCl_2$, $Cu(NO_3)_2$, or $Cu(CH_3COO)_2$ to obtain Cu(II)-ZSM-5 and subsequent reduction with CO has been used as a means for producing Cu-(I)-ZSM-5. The maximum level of exchange attained by this means such that all Cu(II) cations are located at cation-exchange positions is Cu/Al $\approx$ 0.5.[5−18] While higher values of Cu/Al > 0.5 have been achieved by this method, the fraction of Cu(II) present as nanoparticles of CuO increases with the level of overexchange.[5,19] Attempts to introduce Cu^+ cations by aqueous exchange using a solution containing Cu^+ cations have also been attempted, but here too exchange levels above 0.5 could not be achieved.[20] Exchange levels close to unity have been obtained, though, by solid-state ion exchange (SSIE) of the H form of the zeolite using CuCl as the precursor.[13,21−34] A potential problem with this approach, though, is occlusion of unexchanged CuCl in the zeolite pores. This problem can be minimized by raising the sublimation temperature to 1023 K toward the end of the exchange process.[33] Cu K-edge X-ray absorption near-edge structure (XANES) data show that the cations in Cu(I)-ZSM-5 prepared in this manner are exclusively Cu^+, and analysis of Cu extended X-ray absorption fine structure (EXAFS) data shows that the Cu^+ is both doubly and triply coordinated to O atoms, resulting in an average coordination number of ∼2.5 and an average Cu−O bond distance of 1.98 Å.

Attempts to differentiate the properties of Cu^+ cations in different exchange sites located in ZSM-5 have been made using both experimental and theoretical methods. A number of researchers have attempted to do this by infrared spectroscopy of adsorbed CO.[5,19,32,35−39] Most investigators have concluded that if is not possible to distinguish Cu^+ cations in different exchange sites by this means because the bands for C−O vibrations lie within a narrow range of frequencies (2157−2159 cm^{-1});[32,35,37] however, there have been several attempts to deconvolute the single band into two peaks and assign them to different types of Cu^+ sites.[19,36] Theoretical studies of CO adsorption in Cu(I)-ZSM-5 suggest that there are three types of Cu^+ cations.[40−42] The first are those located at charge-exchange sites occurring at the intersections of the straight and sinusoidal channels in the zeolite, the I2 sites, for which the heat of CO adsorption is calculated to be from 42 to 44 kcal/mol,[40] 32 kcal/mol,[41] and 29 kcal/mol.[42] The second type of Cu^+ cations occur in cation-exchange sites located on the channel walls, such as Z6 sites, for which the heat of CO adsorption is calculated to be 36 kcal/mol,[40] 26 kcal/mol,[41] and 23 kcal/mol.[42] The third type of Cu^+ cations locate in the vicinity of an Al pair, for which the heat of CO adsorption is calculated to be 29 kcal/mol,[40] 20 kcal/mol,[41] and 18 kcal/mol.[42] Evidence for the presence of three types of Cu^+ sites for CO adsorption in Cu(I)-ZSM-5 has been proposed based on the deconvolution of CO TPD spectra.[40−42]

* To whom correspondence should be addressed: E-mail: xiaobo@berkeley.edu (X.Z.); bell@cchem.berkeley.edu (A.T.B.).

10.1021/jp072016i CCC: $37.00
Published on Web 08/17/2007

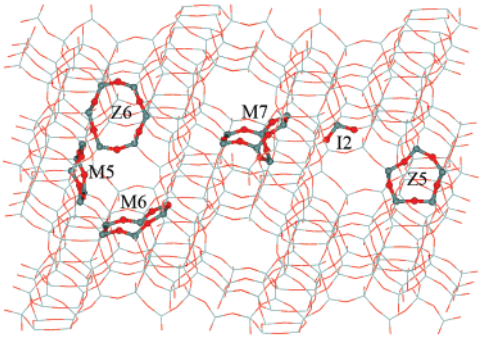

Figure 1. Cu^+ sites in ZSM-5 investigated in this work.

The aim of the present investigation was to carry out a thorough investigation of the geometry of Cu^+ cations exchanged into each of the possible charge-exchange sites in ZSM-5 and to characterize the adsorption of CO on Cu^+ at each of these sites. The latter effort included determination of changes in the coordination of Cu^+ with respect to O atoms in the zeolite framework, the heats of CO adsorption, and the C−O vibrational frequencies. The results of these calculations were then compared with experimental data obtained from this laboratory for fully exchanged Cu(I)-ZSM-5 that had been characterized by XANES, EXAFS, and infrared spectroscopy of adsorbed CO.[34,43]

Computational Methods

The charge-exchange sites in ZSM-5 at which Cu^+ can be coordinated are shown in Figure 1. The site notations shown in this figure are identical to that introduced by Nachtigallova et al.[44] Structures in which Cu^+ is bonded to two framework oxygen atoms connected to a tetrahedrally coordinated Al atom are referred to as I2 sites. These sites occur when an Al atom replaces a Si atom at the intersection of the straight and sinusoidal channels. The sites where Cu^+ is located in five- or six-membered rings of the main (straight) channels of ZSM-5 are referred to as M5 and M6 sites, respectively. The sites where Cu^+ is located in the basket structures formed by two fused five-membered rings of the main channels are referred to as M7 sites. Likewise, the sites containing Cu^+ situated in the five- or six-membered ring structures of the ZSM-5 sinusoidal channels are referred to as Z5 and Z6 sites. It is noted further that for each of the ring structures Al atoms may be located in different positions. Thus, for each ring structure, it is necessary to consider the effects of placing Al atoms at different T sites on the coordination of Cu^+ cations before and after CO adsorption.

Each Cu^+ cation and the associated charge-exchange site were represented by a cluster formed by cutting out a small portion of the catalyst lattice near the charge-exchange site. The Accelrys Material Studio suite of programs was used for this purpose.[45] Si atoms located at the cluster edge were fixed in their crystallographic positions, and all dangling bonds were saturated with H atoms located 1.5 Å from each terminal Si atom and oriented in the direction of the next tetrahedral atom. A 5T cluster was used to describe I2, Z5, and M5 sites, a 6T cluster was used to describe Z6 and M6 sites, and a 7T cluster was used to describe M7 sites.

All density functional theory (DFT) calculations were performed with the GAUSSIAN03 software package.[46] Geometries were optimized at the B3LYP/6-31++G** level. Cu was described using the cc-PVTZ basis set of Balabanov et al.[47] Frequency calculations were carried out to confirm the stability of all ground-state structures. The basis set superposition error (BSSE) was calculated using the counterpoise correction method.[48,49] Zero-point vibrational energies (ZPVEs) were obtained from harmonic vibrational frequencies calculated at the B3LYP/6-31++G** level.

TABLE 1: Comparison of Calculated and Experimental Successive CO Dissociation Energies (kcal/mol) for $Cu^+(CO)_n \rightarrow Cu^+(CO)_{n-1} + CO$, $n = 1, 2, 3, 4$

	calcd	Davidova et al.[40]	exptl[50]
$n = 1$	37	39	36
$n = 2$	38	37	41
$n = 3$	18	17	18
$n = 4$	13	15	13

To validate the choice of computational methods, successive CO dissociation energies for the reaction $Cu^+(CO)_n \rightarrow Cu^+(CO)_{n-1} + CO$ ($n = 1, 2, 3, 4$) were calculated and compared with the experimental measurement reported by Meyer et al.[50] and the theoretical results of Davidova et al.[40] As shown in Table 1, the calculated CO dissociation energies are in excellent agreement with those reported experimentally, the largest deviation being less than 3 kcal/mol. The differences between the dissociation energies obtained in this study and that reported by Davidova et al.[40] are due to the choice of the basis set used for Cu. The cc-PVTZ Cu basis set was used in the present work, whereas Davidova et al.[40] used the double-ξ-plus-polarization-function basis set.

DFT calculations of the C−O vibrational frequency of CO adsorbed on Cu(I)-ZSM-5 based on a cluster representation of the adsorption site predict a mode that is higher than that observed for gas-phase CO, but the magnitude of this blue shift is about 50 cm^{-1} larger than that seen experimentally.[40] Studies of this issue by Nachtigall and co-workers[51] have suggested that the error can be associated with the proper description of the CO vibrational dynamics including anharmonic effects, the level of theory used in the quantum chemical methods used for the electronic structure calculations, and the size and topology of the zeolite model.[52−55] Nachtigall and co-workers[52,53] showed that ν_{CO} could be determined with near-spectroscopic accuracy by use of a scaling method based on the linear correlation of vibrational frequencies and bond length. The parameters in this model were determined from a correlation of C−O stretching frequencies determined at the CCSD(T)/BSI level and the C−O bond length determined at the B3LYP, BLYP, or MP2 level for a series of model compounds containing Cu(I) cations and CO. When applied to CO adsorbed at Cu(I) cations located at I2, Z6, M6, and M7 exchange in Cu(I)-ZSM-5 sites, this scaling approach predicts CO frequencies in the range of 2159−2170 cm^{-1} provided that the DFT calculations are carried out using sufficiently large clusters (i.e., 12−23 T atoms).

While the scaling approach developed by Nachtigall and co-workers represents a significant advance, the use of this method requires that C−O bond distance are calculated using large clusters and the QM-Pot program for the reported scaling parameters to be valid. For these reasons, we have chosen a simpler scaling approach that is based on comparison of the calculated CO frequencies for Cu(CO)Cl and $Cu(CO)_2Cl$ with those reported experimentally.[56] As shown in Table 2, the experimental C−O vibrational frequency of Cu(CO)Cl is reported by Shao et al. to be 2156.8 cm^{-1}.[56] This CO frequency calculated at the B3LYP/6-31++G** level is 2205.8 cm^{-1}. Similarly, for $Cu(CO)_2Cl$, the experimentally observed CO vibrational frequencies are 2131.6 and 2165.8 cm^{-1},[56] whereas the corresponding calculated values are 2179.3 and 2214.7 cm^{-1}.

TABLE 2: Calculated/Experimental CO Vibration Frequencies (cm^{-1}) of Cu(CO)Cl and $Cu(CO)_2Cl$

	B3LYP/6-31++G**	exptl[56]	scaling factor
Cu(CO)Cl	2205.8	2156.8	0.978
$Cu(CO)_2Cl$	2179.3, 2214.7	2131.6, 2165.8	0.978, 0.978

The scaling factor used for the present study, 0.978, was obtained by taking the ratio of the calculated to the experimental vibrational frequency.

Results

I2 cation-exchange sites are located at the intersection of the main and sinusoidal channels. Since these sites can involve Al in the T1, T2, T3, T5, T6, T7, or T12 sites of the MFI lattice, calculations were performed with Al in each of these positions. Parts a and b of Figure 2 illustrate the geometry of this site before and after CO adsorption for the case where Al is situated in the T12 position. Prior to CO adsorption, Cu^+ coordinates two of the four framework oxygen atoms bonded to the Al atom in the T12 position. Table 3 shows that the Cu−O bond distances in this case are 2.00 and 2.02 Å. Following CO adsorption, the position of the Cu^+ remains the same, as do the lengths of the Cu−O bonds, 2.00 and 2.02 Å. The Cu−C and C−O bond distances are 1.81 and 1.14 Å, respectively. The calculated CO adsorption energy is 32.6 kcal/mol, and the scaled C−O stretching frequency is 2150 cm^{-1}. Table 3 shows that placement of Al at other T positions does not alter either the CO adsorption energy or the C−O stretching frequency significantly.

To determine whether cluster size affected the results of the present investigation, a large 12T cluster including a 10-membered ring representing the main channel of ZSM-5, as shown in Figure 2c, was examined. Prior to CO adsorption, Cu^+ bonds to two framework O atoms connected to an Al atom in the T12 position. The calculated Cu−O distances are 1.99 and 2.03 Å. Following CO adsorption, the Cu−O distances remain unchanged. The calculated CO adsorption energy is 31.2 kcal/mol. A comparison of the calculated Cu−O bond distances, CO binding energies, and C−O vibration frequencies for CO adsorption on Cu^+ located in I2 sites determined using a 5T cluster and a 12T cluster are shown in Table 4. The geometric parameters calculated using the large 12T cluster are not significantly different from those obtained using the 5T cluster. The calculated CO adsorption energy and C−O vibration frequency are also very similar. On the basis of this comparison, we conclude that CO adsorption on Cu^+ cations in I2 sites could be determined reliably using a 5T cluster.

The Z5 sites are located in five-membered rings located on the walls of the sinusoidal channels of ZSM-5. The Al atoms in these rings can occupy T2, T3, T4, T5, and T6 positions. Figure 3 shows the Z5 cluster model (with Al at the T4 position) before and after CO adsorption. The peripheral H atoms are omitted from the figure for clarity. Before CO adsorption, Cu^+ forms three bonds with framework O atoms with distances of 2.06, 2.10, and 2.16 Å. After CO adsorption, the Cu^+ moves from its original position by 0.3 Å and the distances of three Cu−O bonds become 2.06, 2.09, and 2.45 Å. The calculated CO adsorption energy is 28.1 kcal/mol, and the C−O vibrational frequency is 2151 cm^{-1}. As seen in Table 3, placement of Al substitution into the T3 and T6 positions does not alter significantly either the CO adsorption energy or the C−O vibrational frequency.

Z6 sites occur in six-membered rings located on the walls of the sinusoidal channels of the zeolite. The Al atoms in the ring occupy the T1, T5, T4, T7, T11, and T10 positions. For Al in the T10 position, Cu^+ coordinates with three framework oxygen atoms with distances of 2.03, 2.06, and 2.09 Å, as shown in Figure 4. After CO adsorption, Cu^+ migrates from its original position and bonds with only two framework oxygen atoms in the Al tetrahedron. The Cu−O distances are now 2.03 and 2.02 Å. The calculated CO stretching frequency is 2151 cm^{-1}, and

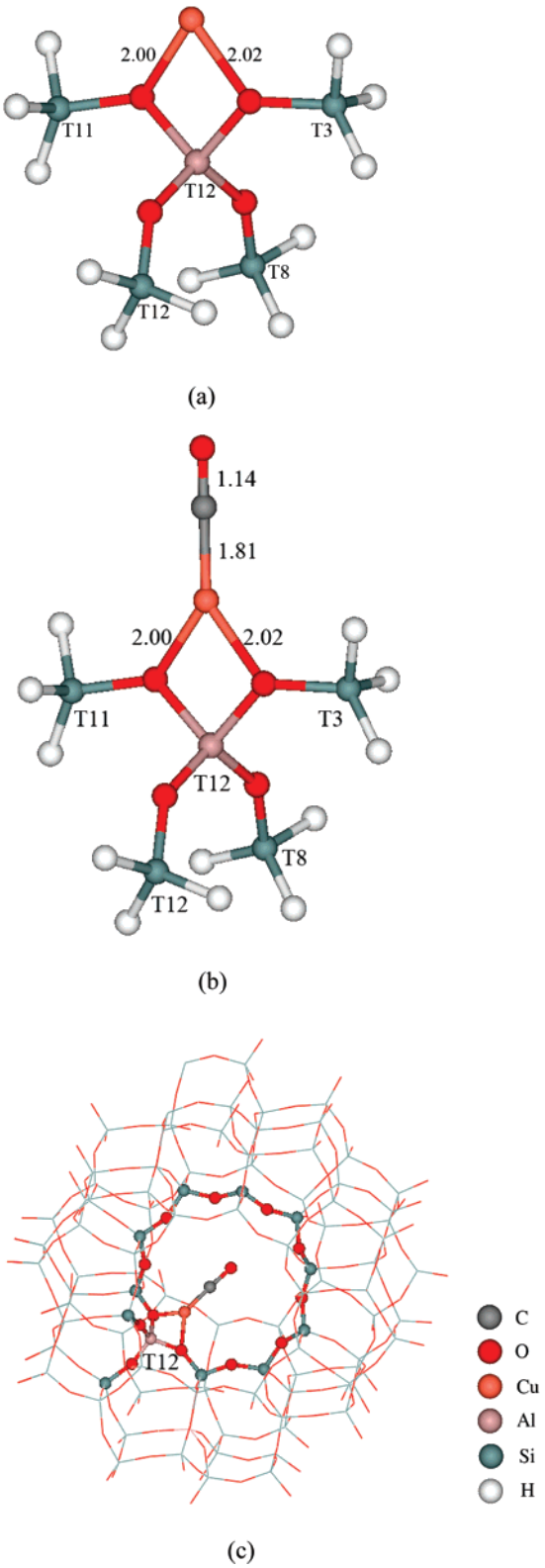

Figure 2. I2 site of CuZSM-5 (Al at the T12 position): 5T cluster before CO adsorption (a), 5T cluster after CO adsorption (b), and 10-membered-ring cluster after CO adsorption (c).

TABLE 3: Summary of the Calculated Cu−O Coordination Numbers (CNs),[a] Distances, and CO Adsorption Energies and Comparison with Experimental Results

	T sites involved	Al position	CN(Cu−O) before CO ads	CN(Cu−O) after CO ads	*R*(Cu−O) (Å) before CO ads	*R*(Cu−O) (Å) after CO ads	E_{ads} (kcal/mol)	ν(C−O) (cm^{-1})
I2	T2−T1−T5	T1	2	2	2.02, 2.07	2.01, 2.08	31.3	2155
	T6−T2−T1	T2	2	2	2.07, 2.08	2.06, 2.09	30.3	2157
	T2−T3−T6	T3	2	2	2.02, 2.05	2.00, 2.04	32.8	2158
	T4−T5−T6	T5	2	2	2.00, 2.12	1.98, 2.15	30.3	2153
	T5−T6−T9	T6	2	2	2.03, 2.04	2.02, 2.04	31.6	2154
	T4−T7−T11	T7	2	2	2.03, 2.07	2.02, 2.08	32.2	2156
	T11−T12−T3	T12	2	2	2.00, 2.02	2.00, 2.02	32.6	2150
Z5	T2−T3−T4−T5−T6	T3	3	3	2.05, 2.42, 2.13	2.08, 2.24, 2.33	28.0	2155
		T4	3	3	2.06, 2.10, 2.16	2.06, 2.09, 2.45	28.1	2151
		T6	3	2	2.04, 2.24, 2.33	2.10, 2.21	27.3	2153
Z6	T1−T5−T4−T7−T11−T10	T10	3	2	2.03, 2.06, 2.09	2.02, 2.03	24.9	2151
		T11	3	3	1.96, 2.04, 2.49	1.97, 2.48. 2.49	25.3	2155
		T4 and T10	4	3	2.02, 2.28, 2.12, 2.26	2.03, 2.38, 2.36	17.3	2142
M5	T2−T3−T6−T9−T8	T2	3	3	2.06, 2.17, 2.32	2.09, 2.19, 2.39	28.3	2156
		T6	3	2	2.05, 2.25, 2.34	2.09, 2.16	28.2	2154
M6	T7−T11−T12−T12−T11−T7	T11	4	2	2.07, 2.11, 2.36, 2.49	2.01, 2.04	26.8	2152
		T11 and T11	3	2	2.02, 2.16, 2.10	1.97, 2.09	23.4	2143
		T7 and T12	3	2	2.01, 2.24, 2.26	2.05, 2.14	25.2	2150
		T7 and T7	4	2	2.01,2.29,2.43, 2.46	1.98, 2.26	25.0	2147
M7	T1−T2−T8−T7−T11−T5, T4	T4	3	2	2.12, 2.26, 2.46	2.02, 2.11	21.1	2178
		T1 and T7	4	2	2.17, 2.18, 2.24, 2.35	2.01, 2.06	20.1	2159

[a] A Cu−O distance of 2.5 Å is used to decided whether Cu bonds with O.

TABLE 4: Calculated Geometry Parameters for CO Adsorption (Distances, Å; Angles, deg), Binding Energies (kcal/mol), and C−O Vibration Frequencies (cm^{-1}) on the I2 Site Calculated Using a 5T Cluster and a 10-Membered-Ring 12T Cluster

	5T cluster		10-membered-ring 12T cluster	
	before CO ads	after CO ads	before CO ads	after CO ads
R(Cu−O1)	2.00	2.00	1.99	1.99
R(Cu−O2)	2.02	2.02	2.03	2.03
R(Cu−Al)	2.77	2.80	2.80	2.83
R(Cu−C)	1.81		1.81	
R(C−O)	1.14		1.14	
A(Cu−C−O)	179.98		179.68	
E_{ads}	32.6		31.2	
ν(CO)[a]	2150		2151	

[a] Frequency scaled by 0.978.

the calculated CO adsorption energy is 24.9 kcal/mol. Only small changes in both the CO adsorption energy and the C−O stretching frequency occur when the position of the Al atom is changed (see Table 3).

M5 sites are contained in five-membered rings located on the walls of the main (straight) channels of ZSM-5. The T atoms in the ring occupy T2, T3, T6, T9, and T8 positions. For Al in the T2 position, the calculated structures before and after CO adsorption are shown in Figure 5. Cu^+ coordinates with three oxygen atoms before and after CO adsorption. The calculated CO adsorption energy is 28.3 kcal/mol, and the C−O stretching frequency is 2156 cm^{-1}. Shifting Al to the T6 position alters the calculated CO adsorption energy and C−O vibrational frequency very little.

M6 sites occur in six-membered rings located on the walls of the main channels of the zeolite. The T atoms in such rings occur at T7, T12, T11, T12, T7, and T11 positions. For Al at the T11 position, calculated structures before and after CO adsorption are shown in Figure 6. Prior to CO adsorption, Cu^+ forms four bonds with framework oxygen atoms, with distances of 2.07, 2.11, 2.36, and 2.49 Å. Upon CO adsorption, the Cu−O coordination of Cu^+ decreases to 2 and the Cu−O bond distances change to 2.01 and 2.04 Å. The calculated CO vibrational frequency in this case is 2152 cm^{-1}, and the calculated CO adsorption energy is 26.8 kcal/mol.

M7 sites occur in the basketlike structures formed by fusing two five-membered rings involving T4−T7−T8−T2−T1 and T4−T7−T11−T5−T1 atoms. The structures of Cu^+ exchanged into M7 sites before and after CO adsorption are shown in Figure 7. For Al in the T4 position, Cu^+ is coordinated with three framework oxygen atoms, only one of which is bonded to Al. The Cu−O distances are 2.12, 2.26, and 2.46 Å. Significant movement of the Cu^+ cation occurs upon CO adsorption. Cu^+ now bonds to two framework oxygen atoms, neither of which is connected to the Al atom, and the Cu−O distances are 2.02 and 2.11 Å. The calculated CO stretching frequency is 2178 cm^{-1}, and the calculated CO adsorption energy is 21.1 kcal/mol. The adsorption energy is much lower than that for Cu^+ in I2 sites because Cu^+ bonds to two oxygens that are not bonded directly to an Al atom.

Si/Al Ratio Effects on CO Adsorption. Table 3 also shows the results of calculations in which two Al atoms are introduced into M6, M7, and Z6 charge-exchange sites. The appearance of Al in the next-nearest-neighbor position in ZSM-5 becomes possible when the Si/Al ratio approaches 10, the lower limit for this zeolite.[57]

Structures of CO adsorbed on a Cu^+ cation located in an M6 cation-exchange site containing two Al atoms are shown in Figure 8. Depending on the positions of the two Al atoms, the cluster structures are referred to as symmetrical if the Al atoms are located at the T11 and T11 positions, distorted if the Al atoms are located at the T7 and T12 positions, and nonsymmetrical if the Al atoms are located at the T7 and T7 positions.[58] Since the extra Al brings a negative charge to the cluster, a proton is added to compensate this charge. Upon CO adsorption, the Cu−O coordination number changes from 3 to 2 and significant migration of Cu^+ from its original position occurs. The calculated CO adsorption energies range from 23.4 to 25.2 kcal/mol, and the corresponding C−O stretching frequencies are 2143 and 2150 cm^{-1}.

The structures before and after CO adsorption on Cu^+ exchanged into M7 and Z6 sites containing a pair of Al atoms

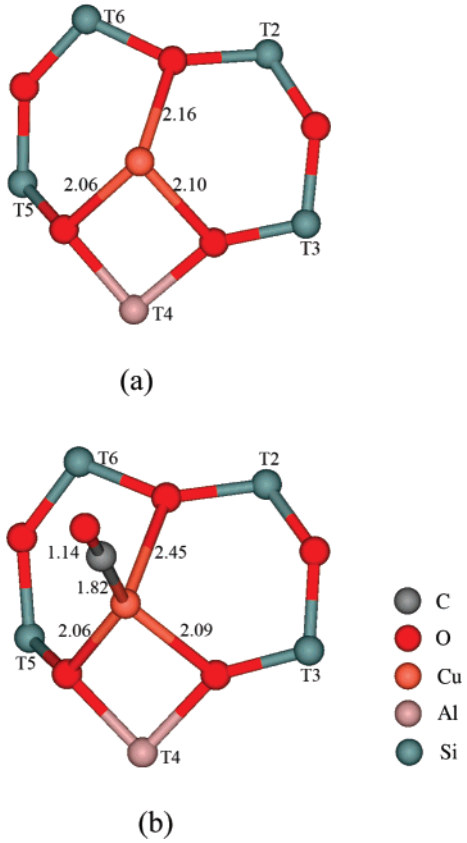

Figure 3. Z5 site of CuZSM-5 (Al at the T4 position) before (a) and after (b) CO adsorption.

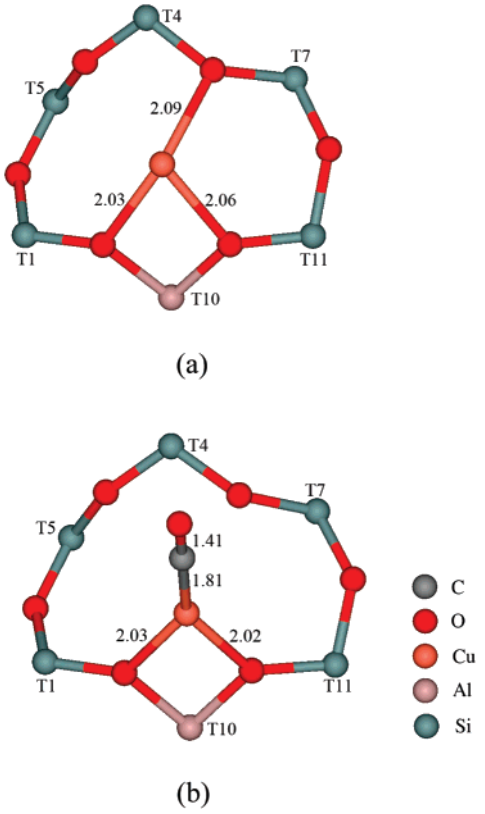

Figure 4. Z6 site of CuZSM-5 (Al at the T12 position) before (a) and after (b) CO adsorption.

are shown in Figures 9 and 10. For two Al atoms in an M7 site, the Cu−O coordination number changes from 4 to 2 after CO adsorption. The calculated CO adsorption energy is 20.1 kcal/mol, and the C−O stretching frequency is 2159 cm^{-1}. For two Al atoms in a Z6 site, the Cu−O coordination number changes from 4 to 3 after CO adsorption. The calculated CO adsorption energy for this case is 17.3 kcal/mol, and the C−O stretching frequency is 2142 cm^{-1}.

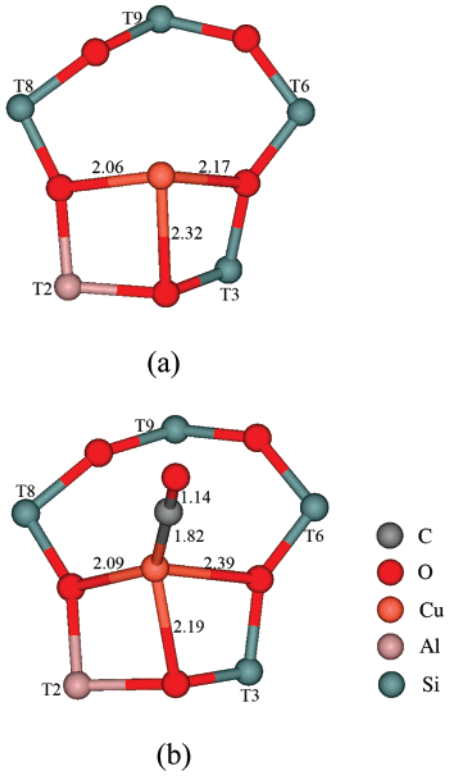

Figure 5. M5 site of CuZSM-5 (Al at the T2 position) before (a) and after (b) CO adsorption.

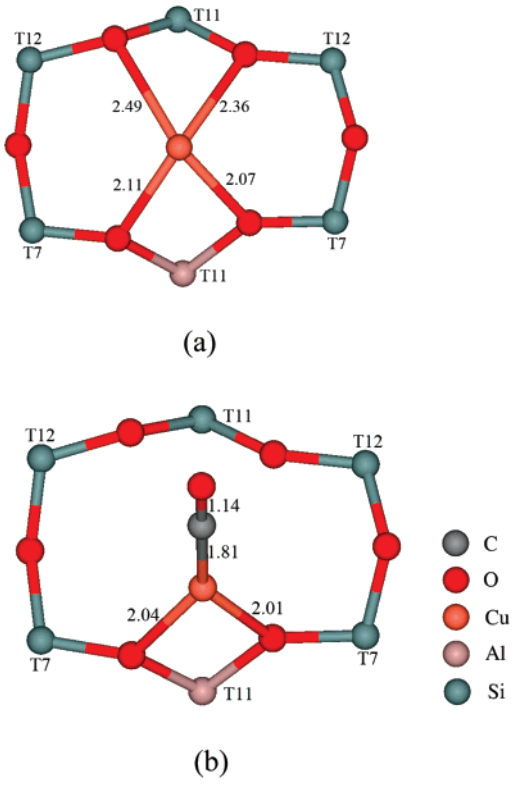

Figure 6. M6 site of CuZSM-5 (Al at the T11 position) before (a) and after (b) CO adsorption.

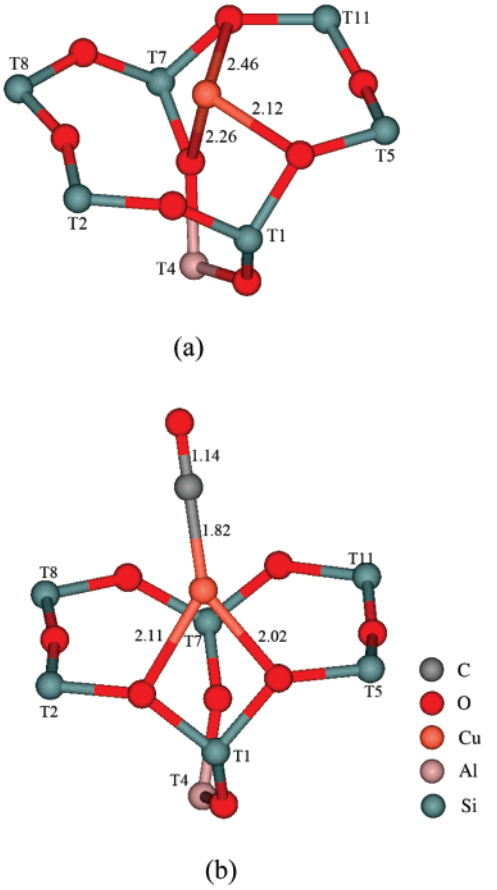

Figure 7. M7 site of CuZSM-5 (Al at the T4 position) before (a) and after (b) CO adsorption.

Discussion

The following issues are examined in light of the results presented above: the distribution of Cu^+ cations among different types of charge-exchange sites in Cu(I)-ZSM-5, the possibility of discerning different types of CO adsorption sites by either infrared spectroscopy or temperature-programmed desorption spectroscopy of adsorbed CO, and the effects of CO adsorption on the coordination of Cu^+ with respect to O atoms in the zeolite framework.

Previous theoretical studies have revealed that only relatively small differences in energy occur when Al is moved from one to another of the 12 possible T positions in the MFI framework.[44,59,60] This suggests that during the synthesis of ZSM-5 Al atoms may distribute randomly among all of the T sites. The probability of finding two Al atoms in five- and six-membered rings has also been examined previously.[57] For Si/Al = 12, the fraction of five- and six-membered rings with two Al atoms will be 3.3% and 5.4%, respectively, and for Si/Al = 24, the fraction of five- and six-membered rings with two Al atoms will be 0.9% and 0.2%, respectively. These calculations suggest that the probability of finding two Al atoms in the M5, M6, Z5, and Z6 charge-exchange sites is relatively small for ZSM-5 prepared with Si/Al ratios of ≥ 12.

EXAFS studies of fully exchanged Cu(I)-ZSM-5 prepared by SSIE using CuCl as the source of Cu^+ have shown that the average Cu−O coordination number is ~2.5 and the average Cu−O bond distance is 1.98 ± 0.02 Å.[34] Similar EXAFS results were presented previously by Lamberti et al.[32] A coordination number of greater than 2 suggests that Cu^+ exchanges into sites for which the coordination is 2 and 3. Reference to Table 3 indicates that a coordination number of 2 is characteristic of I2 exchange sites, whereas a coordination number of 3 is characteristic of Z5, Z6, M5, M6, and M7 exchange sites containing one Al atom. Thus, an average Cu−O coordination number of 2.5 could be achieved by assuming that 50% of the Cu^+ cations are located in I2 exchange sites and the remaining 50% in Z5, Z6, M5, M6, and M7 exchange sites. To test this hypothesis, simulated EXAFS patterns were calculated using the FEFF8 code,[61,62] and the results were compared with experimental results obtained in our laboratory.[7] FEFF8 is a program for ab initio multiple scattering calculations of X-ray absorption fine structure (XAFS) and XANES spectra for clusters of atoms. The code yields scattering amplitudes and phases used in many modern XAFS analysis codes, as well as various other properties. Figure 11 shows simulated EXAFS patterns for Cu^+ in I2 and Z6 sites. The location of the Al atom in a particular type of site has little influence on the simulated EXAFS pattern, and

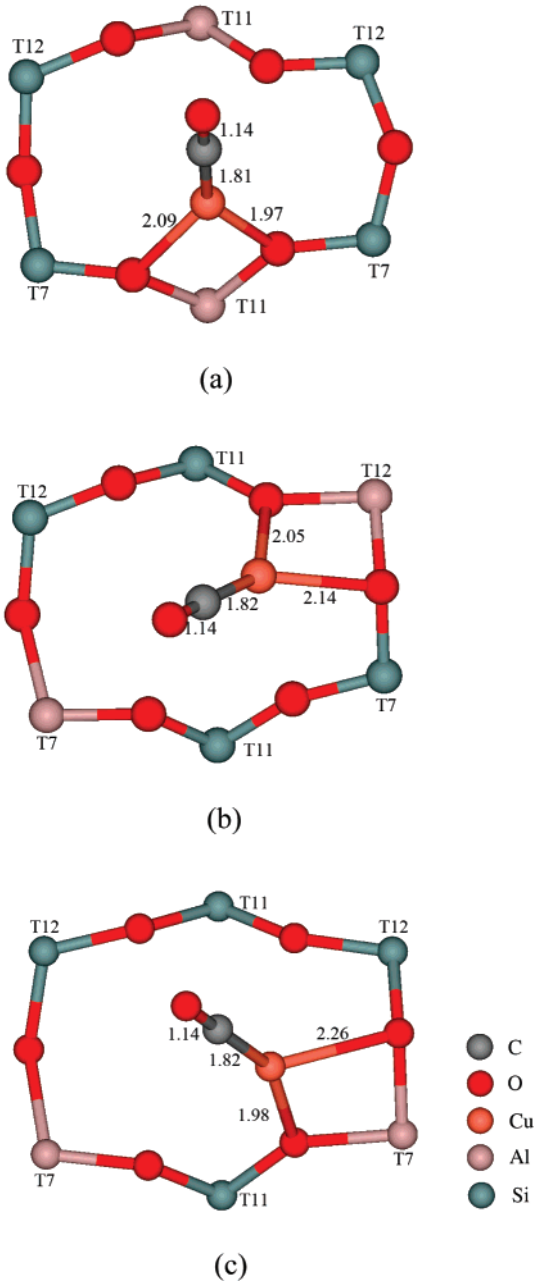

Figure 8. CO adsorption on the M6 site of CuZSM-5 (two Al atoms): (a) symmetrical structure (Al at T11 and T11); (b) distorted structure (Al at T7 and T12); (c) nonsymmetrical structure (Al at T7 and T7).

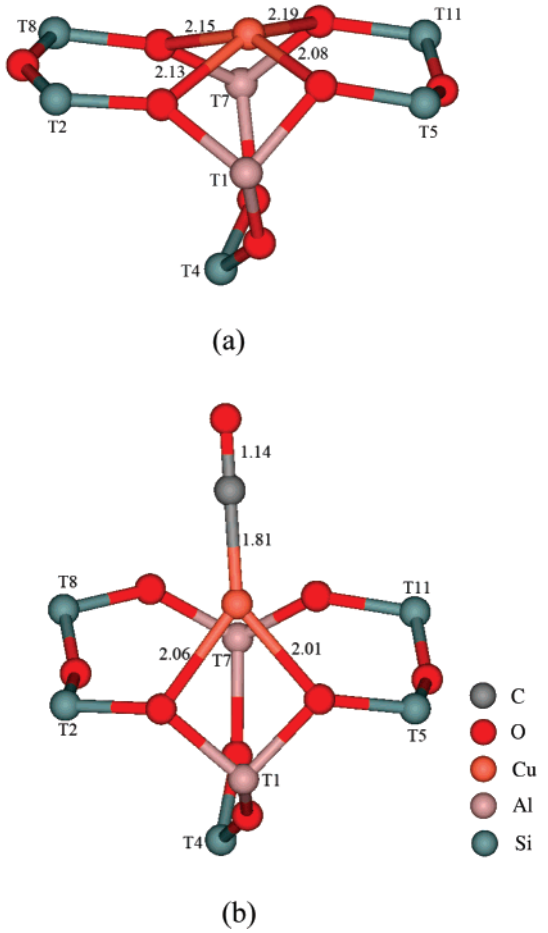

Figure 9. M7 site of CuZSM-5 (Al at the T1 and T7 positions) before (a) and after (b) CO adsorption.

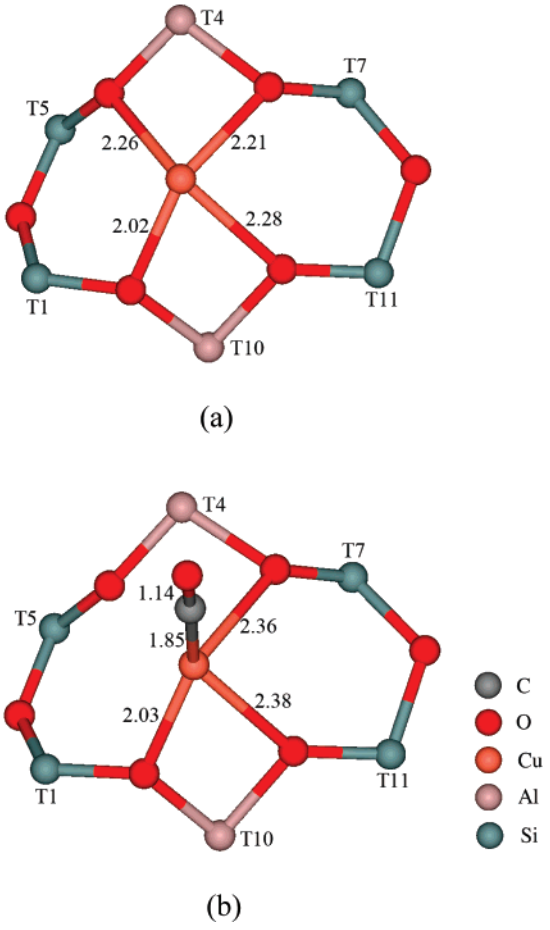

Figure 10. Z6 site of CuZSM-5 (Al at the T4 and T10 positions) before (a) and after (b) CO adsorption.

the EXAFS patterns for Cu^+ in Z5, M5, M6, and M7 exchange sites are very similar to that for Cu^+ in the Z6 site. The right-hand panel of Figure 11 shows that a reasonably close match of the simulated to the experimentally observed EXAFS pattern can be obtained assuming that 70% of the Cu^+ is located in I2 sites and the balance in Z6 sites.

In Figure 12, the vibrational frequencies for adsorbed CO and the energy of CO adsorption are plotted for each of the entries listed in Table 3. Different charge-exchange sites are identified by a symbol, and sites containing one Al atom are designated by a solid symbol, whereas sites containing two Al atoms are designated by an open symbol. It is evident that CO adsorbed on Cu^+ cations located at I2 cation-exchange sites has C−O stretching frequencies between 2150 and 2158 cm^{-1} and CO adsorption energies between 30.0 and 32.8 kcal/mol. These values are in good agreement with previous calculations reported by other researchers.[42,63] CO adsorbed on Cu^+ cations located at Z6, M5, and M6 exchange sites has C−O vibrational frequencies between 2150 and 2156 cm^{-1} and CO adsorption energies between 24.5 and 28.0 kcal/mol. CO adsorbed on Cu^+ located at Z6, M6, and M7 sites containing two Al atoms exhibit calculated CO adsorption energies that lie between 17.3 and 25.2 kcal/mol, whereas the C−O vibrational frequencies associated with such adsorption sites lie between 2142 and 2159 cm^{-1}. Interestingly, CO adsorbed on Cu^+ located at an M7 site containing one Al atom also has a calculated CO adsorption energy in the same range, but an unusually high C−O vibrational frequency of 2178 cm^{-1}.

As noted above, ZSM-5 for which the Si/Al ratio is ≥12, as is the case for samples investigated experimentally, is projected to contain only a very small percentage of five- and six-membered rings (viz., Z5, Z6, M5, M6, and M7 cation-exchange sites) containing two Al atoms. Therefore, all of the points appearing as open circles in Figure 12 are unlikely to be accessible to experimental observations. It is also likely that the fraction of Al present in M7 cation-exchange sites containing one Al atom is small. Following this logic, our calculations would lead to the expectation that the infrared spectrum of adsorbed CO should be dominated by features occurring between 2150 and 2158 cm^{-1} due to CO adsorbed on Cu^+ cations associated with I2, Z5, Z6, M5, and M6 sites and exhibit only a weak feature at 2178 cm^{-1} due to CO adsorbed on Cu^+ cations associated with M7 sites. Figure 13 shows that these projections are in very good agreement with what is observed experimentally in our laboratory.[43] It is noted that the main feature centered at 2151 cm^{-1} in the infrared spectrum of adsorbed CO observed experimentally is comprised of two or more closely overlapping components, which means that it is not feasible to use infrared spectroscopy to discern different adsorption centers in Cu(I)-ZSM-5. This conclusion agrees with that of Bludsky et al.[52] but contradicts that of Kumashiro et al.,[36] who concluded that the infrared peak for adsorbed CO could be deconvoluted into two bands located at 2151 and 2159 cm^{-1}, which they ascribed to CO on Cu^+ coordinated to two and three framework O atoms, respectively. The results of the present study (see Table 3 and Figure 12) demonstrate that such an assignment cannot be made since the calculated C−O vibrational frequencies for CO adsorbed on Cu^+ coordinated to two O atoms (i.e., I2 sites) and three O atoms (i.e., Z5, Z6, M5, and M6 sites) overlap.

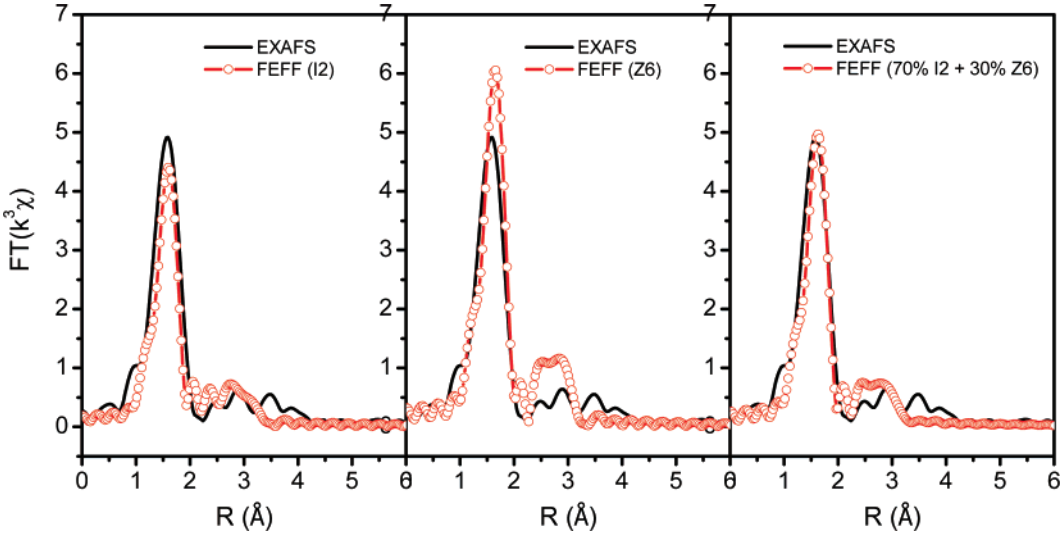

Figure 11. Comparison of the experimentally determined EXAFS spectra of CuZSM-5 with FEFF simulation spectra of the I2 structure model (left), Z6 structure model (middle), and 70% I2 + 30% Z6 structure model (right).

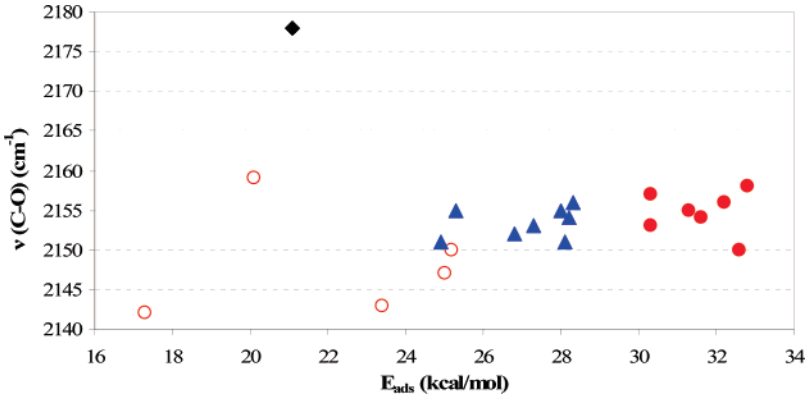

Figure 12. Correlation of calculated CO stretching frequencies with CO adsorption energies on various CuZSM-5 sites (red solid circles refer to I2 sites, red open circles refer to ring sites (M6, M7, and Z6 sites) with two Al atoms, blue triangles refer to ring sites (M5, M6, Z5, and Z6 sites) with one Al atom, and the black tilted square refers to the M7 site).

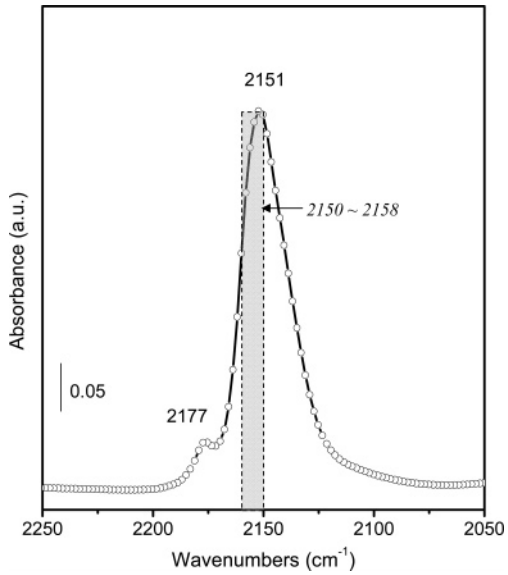

Figure 13. Comparison of the calculated and experimental CO vibrational spectra on CuZSM-5.

The infrared spectrum shown in Figure 13 also exhibits a weak band at 2177 cm^{-1}. This band has been assigned previously to the asymmetric stretching of C−O bonds in dicarbonyl species.[33] However, the results shown in Table 3 suggest that an alternative assignment could be to CO adsorbed on Cu^+ cations associated with M7 exchange sites. To clarify this issue, calculations were performed to determine the adsorption energy and the vibrational frequencies for dicarbonyls formed on Cu^+ cations associated with I2 and Z6 exchange sites. The results of these calculations are presented in Table 5. As noted there, the adsorption energy for addition of a second CO to a monocarbonyl on a Cu^+ located at an I2 or Z6 exchange site is 4.8 or 1.5 kcal/mol, respectively. The C−O vibrational frequencies are 2143 and 2176 cm^{-1} for dicarbonyls formed on Cu^+ cations at I2 sites and 2146 and 2178 cm^{-1} for dicarbonyls formed on Cu^+ cations at Z6 sites. Since the experimental band at 2177 cm^{-1} disappears completely when the temperature of Cu(I)-ZSM-5 is raised from 298 to 373 K, its assignment to asymmetric vibrations of a dicarbonyl is more plausible than its assignment to a monocarbonyl species formed on Cu^+ cations associated with M7 sites.

TABLE 5: Calculated Adsorption Energies (kcal/mol) and C−O Vibrational Frequencies (cm^{-1}) of a Dicarbonyl Complex on Cu-ZSM5

site I2 (Al@T12)	CO E_{ads}	32.6	ν(C−O)	2150	
	2CO E_{ads}	4.8	ν(C−O)	2143	2176
site Z6 (Al@T10)	CO E_{ads}	24.9	ν(C−O)	2151	
	2CO E_{ads}	1.5	ν(C−O)	2146	2178

A further observation deducible from Figure 12 is that the heat of adsorption for CO adsorbed on Cu^+ cations associated with I2 sites is not uniquely defined but, in fact, exhibits a range

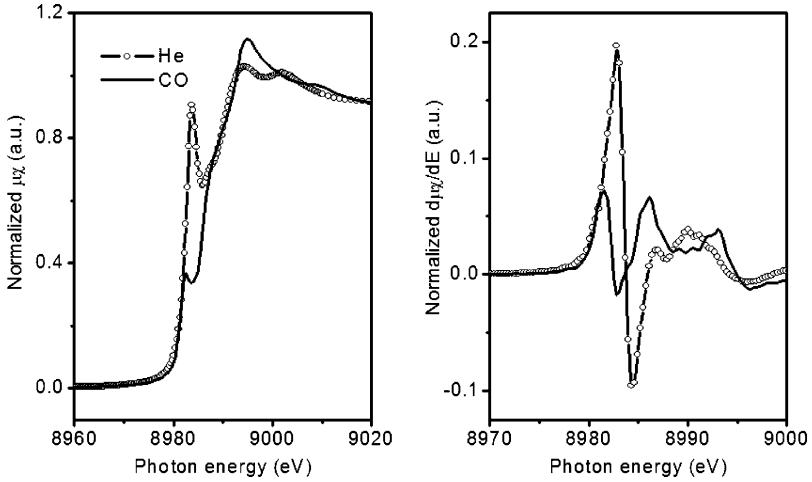

Figure 14. XANES spectra of CO adsorption on Cu-ZSM-5 and their derivative curves.

of values lying between 30 and 33 kcal/mol. Likewise, the heat of CO adsorption on Cu^+ cations associated with Z5, Z6, M5, and M6 sites lies in the range of 25−28 kcal/mol. Our finding of a higher heat of adsorption of CO on I2 sites than on Z5, Z6, M5, and M6 sites is qualitatively consistent with the work of Bulànek and Nachtigall and their co-workers,[41] who reported a value of 32 kcal/mol for CO adsorption on Cu^+ at sites on the channel intersections (i.e., I2 sites), a value of 26 kcal/mol for CO adsorption on Cu^+ at sites on the channel walls (i.e., Z5, Z6, M5, and M6 sites), and a value of 20 kcal/mol for CO adsorption on Cu^+ at the vicinity of an Al pair. However, in contrast to the findings of these investigators, our results suggest that it would be difficult to deconvolute experimental TPD spectra into three distinct components clearly identified with these three classes of Cu^+ sites because of the narrow gap in the adsorption energies between the two types of sites. This conclusion is reinforced by the fact that experimentally observed TPD spectra are very broad and lacking in well-defined peaks, which makes their deconvolution into a set of uniquely defined peaks a difficult process.

The results presented in Table 3 and in Figures 2−7 show that the coordination of Cu^+ cations changes upon the adsorption of CO. In all cases, the adsorbed CO increases the total Cu^+ coordination number by 1 because of the Cu−C bond formed; however, for several of the sites (e.g., Z5, Z6) the coordination number of Cu^+ with the O atoms of the zeolite lattice decreases. The net effect in most cases, though, is to increase the total coordination number of Cu^+. Work by Solomon and co-workers[64] has demonstrated that differences in Cu^+ coordination can be ascertained from the height of the preedge feature observed in the XANES spectrum of Cu^+ cations. XANES spectra of a large number of Cu(I) compounds and complexes show that 2-coordinated linear Cu(I) complexes have the highest preedge feature, whereas 3-coordinated T-shaped and trigonal planar Cu(I) complexes have a preedge feature that is 0.63 ± 0.05 smaller than that of linear 2-coordinated complexes and centered at slightly lower energy. 4-Coordinated tetrahedral Cu(I) complexes also have preedge features that are somewhat less intense than that of 2-coordinated linear complexes. These trends suggest that XANES spectra taken before and after CO adsorption on Cu(I)-ZSM-5 should show a change in the coordination of Cu^+.

Figure 14 illustrates XANES spectra taken before and after CO adsorption for the sample of Cu(I)-ZSM-5 used for the experimental results reported in Figures 11 and 13.[7,33] The large resonant peak at 8983.6 eV associated with coordinatively unsaturated Cu^+ is replaced by a shoulder at 8982.4 eV upon CO adsorption. In the first-derivative spectrum, the original peak at 8982.7 eV shown for a He-treated sample disappears completely and is replaced by new features at 8981.5, 8986.1, and 8993.1 eV. Similar changes in the XANES spectrum of Cu(I)-ZSM-5 have been reported by Lamberti et al.[32] and Kushimoro et al.[36] The latter authors proposed that the changes in the XANES spectrum could be attributed to a change in the coordination number of Cu^+ caused by the adsorption of CO. If we assume that 70% of the Cu^+ cations in fully exchanged ZSM-5 are located in I2 charge-exchange sites and 30% of the Cu^+ cations are located in Z6 sites, then reference to Table 3 and Figures 2 and 4 would indicate that the coordination of Cu^+ in the former sites increases from 2 to 3 and in the latter sites it remains at 3 but with a change in coordination symmetry from trigonal planar to T-shaped. On the basis of the work of Solomon and co-workers[64] discussed above, the change in coordination of Cu^+ cations associated with I2 sites should cause a large decrease in the intensity of the preedge feature of the XANES spectrum. Likewise, a decrease in the intensity of the preedge feature should also occur for Cu^+ cations associated with Z6 cation-exchange sites as a consequence of the change in coordination symmetry. Consequently, the results of the present investigation enable a more complete interpretation of the changes in the Cu^+ XANES spectrum of Cu(I)-ZSM-5 observed before and after CO adsorption.

Conclusions

A theoretical investigation of the coordination of Cu^+ in Cu(I)-ZSM-5 and the properties of CO adsorbed on such cations has been carried out using density functional theory. The influences of the structure of the cation-exchange site, the location of the Al in the site, and the number of Al atoms associated with the sites were explored. Cu^+ was found to have 2-fold coordination to framework O atoms when present in I2 exchange sites, 3-fold coordination to framework O atoms when present in M5, M6, M7, Z5, and Z6 exchange sites containing one Al atom, and 4-fold coordination to framework O atoms when present in M6, M7, and M7 exchange sites containing two Al atoms. Comparison of simulated and experimental EXAFS patterns suggests that 70% of the Cu^+ cations in fully exchanged Cu(I)-ZSM-5 are associated with I2 sites and 30% are associated with sites such as Z6. CO adsorbed on Cu^+ cations exchanged into I2 sites have heats of adsorption between 30 and 33 kcal/mol and C−O vibrational frequencies between 2150 and 2158 cm^{-1}, whereas CO adsorbed on Cu^+ cations

exchanged into M5, M6, Z5, or Z6 sites containing one Al atom have heats of adsorption between 25 and 28 kcal/mol and C−O vibrational frequencies between 2151 and 2156 cm^{-1}. The presence of two Al atoms in M6, Z6, and M7 sites results in a noticeable lowering of the heat of CO adsorption and an increase in the C−O vibrational frequency. The overlap of the calculated vibrational frequencies for adsorbed CO suggests that it is not possible to use infrared spectroscopy to identify Cu^+ cations associated with different cation-exchange sites. It is also concluded that it would be difficult to discriminate between Cu^+ in different environments on the basis of TPD spectra of adsorbed CO. Evidence for two types of Cu^+ sites can be obtained, though, from analysis of Cu K-edge EXAFS data. The present calculations also provide evidence for a change in the coordination of Cu^+ with framework O atoms upon CO adsorption. The nature of these changes is consistent with recent observations made by Cu K-edge XANES spectroscopy.

Acknowledgment. This work was supported by the Methane Conversion Corporative Program funded by BP. Computations were carried out on a Dell cluster of the Molecular Graphics and Computation Facility at the University of California, Berkeley. Supercomputer time on the NCSA HP/Convex Exemplar SPP-2000 at the University of Illinois at Urbana-Champaign was provided by the National Computational Science Alliance.

References and Notes

(1) Komatsu, T.; Nunokawa, M.; Moon, I. S.; Takahara, T.; Namba, S.; Yashima, T. *J. Catal.* **1994**, *148*, 427.

(2) Iwamoto, M.; Yahiro, H.; Tanda, K.; Mizuno, N.; Mine, Y.; Kagawa, S. *J. Phys. Chem.* **1991**, *95*, 3727.

(3) Chen, H. Y.; Chen, L.; Lin, J.; Tan, K. L.; Li, J. *Inorg. Chem.* **1997**, *36*, 1417.

(4) Anderson, S. A.; Root, T. W. *J. Mol. Catal. A* **2004**, *220*, 247.

(5) Bulanek, R.; Wichterlova, B.; Sobalik, Z.; Tichy, J. *Appl. Catal., B* **2001**, *31*, 13.

(6) Bolis, V.; Barbaglia, A.; Bordiga, S.; Lamberti, C.; Zecchina, A. *J. Phys. Chem. B* **2004**, *108*, 9970.

(7) Castagnola, N. B.; Kropf, A. J.; Marshall, C. L. *Appl. Catal., A* **2005**, *290*, 110.

(8) Da Costa, P.; Moden, B.; Meitzner, G. D.; Lee, D. K.; Iglesia, E. *Phys. Chem. Chem. Phys.* **2002**, *4*, 4590.

(9) Fanson, P. T.; Stradt, M. W.; Lauterbach, J.; Delgass, W. N. *Appl. Catal., B* **2002**, *38*, 331.

(10) Groothaert, M. H.; Lievens, K.; Leeman, H.; Weckhuysen, B. M.; Schoonheydt, R. A. *J. Catal.* **2003**, *220*, 500.

(11) Hu, S. L.; Reimer, J. A.; Bell, A. T. *J. Phys. Chem. B* **1997**, *101*, 1869.

(12) Kuroda, Y.; Kumashiro, R.; Itadani, A.; Nagao, M.; Kobayashi, H. *Phys. Chem. Chem. Phys.* **2001**, *3*, 1383.

(13) Kuroda, Y.; Yagi, K.; Horiguchi, N.; Yoshikawa, Y.; Kumashiro, R.; Nagao, M. *Phys. Chem. Chem. Phys.* **2003**, *5*, 3318.

(14) Larsen, S. C.; Aylor, A.; Bell, A. T.; Reimer, J. A. *J. Phys. Chem.* **1994**, *98*, 11533.

(15) Neylon, M. K.; Marshall, C. L.; Kropf, A. J. *J. Am. Chem. Soc.* **2002**, *124*, 5457.

(16) Palomino, G. T.; Fisicaro, P.; Bordiga, S.; Zecchina, A.; Giamello, E.; Lamberti, C. *J. Phys. Chem. B* **2000**, *104*, 4064.

(17) Tkachenko, O. P.; Klementiev, K. V.; Koc, N.; Yu, X.; Bandyopadhyay, M.; Grabowski, S.; Gies, H.; Grunert, W. *Stud. Surf. Sci. Catal.* **2004**, *154*, 1670.

(18) Tkachenko, O. P.; Klementiev, K. V.; van den Berg, M. W. E.; Koc, N.; Bandyopadhyay, M.; Birkner, A.; Woll, C.; Gies, H.; Grunert, W. *J. Phys. Chem. B* **2005**, *109*, 20979.

(19) Kuroda, Y.; Yoshikawa, Y.; Kumashiro, R.; Nagao, M. *J. Phys. Chem. B* **1997**, *101*, 6497.

(20) Downing, R. S.; van Amstel, J.; Joustra, A. H. U.S. Patent 4,125,-483, 1978.

(21) Bolis, V.; Bordiga, S.; Graneris, V.; Lamberti, C.; Palomino, G. T.; Zecchina, A. *Stud. Surf. Sci. Catal.* **2000**, *130*, 3261.

(22) Palomino, G. T.; Zecchina, A.; Giamello, E.; Fisicaro, P.; Berlier, G.; Lamberti, C.; Bordiga, S. *Stud. Surf. Sci. Catal.* **2000**, *130*, 2915.

(23) Bolis, V.; Bordiga, S.; Palomino, G. T.; Zecchina, A.; Lamberti, C. *Thermochim. Acta* **2001**, *379*, 131.

(24) Spoto, G.; Zecchina, A.; Bordiga, S.; Ricchiardi, G.; Martra, G.; Leofanti, G.; Petrini, G. *Appl. Catal., B* **1994**, *3*, 151.

(25) Lamberti, C.; Bordiga, S.; Bonino, F.; Prestipino, C.; Berlier, G.; Capello, L.; D'Acapito, F.; Xamena, F.; Zecchina, A. *Phys. Chem. Chem. Phys.* **2003**, *5*, 4502.

(26) Spoto, G.; Bordiga, S.; Ricchiardi, G.; Scarano, D.; Zecchina, A.; Geobaldo, F. *J. Chem. Soc., Faraday Trans.* **1995**, *91*, 3285.

(27) Zecchina, A.; Bordiga, S.; Salvalaggio, M.; Spoto, G.; Scarano, D.; Lamberti, C. *J. Catal.* **1998**, *173*, 540.

(28) Prestipino, C.; Berlier, G.; Xamena, F.; Spoto, G.; Bordiga, S.; Zecchina, A.; Palomino, G. T.; Yamamoto, T.; Lamberti, C. *Chem. Phys. Lett.* **2002**, *363*, 389.

(29) Zecchina, A.; Bordiga, S.; Palomino, G. T.; Scarano, D.; Lamberti, C.; Salvalaggio, M. *J. Phys. Chem. B* **1999**, *103*, 3833.

(30) Lamberti, C.; Palomino, G. T.; Bordiga, S.; Berlier, G.; D'Acapito, F.; Zecchina, A. *Angew. Chem., Int. Ed.* **2000**, *39*, 2138.

(31) Spoto, G.; Bordiga, S.; Scarano, D.; Zecchina, A. *Catal. Lett.* **1992**, *13*, 39.

(32) Lamberti, C.; Bordiga, S.; Salvalaggio, M.; Spoto, G.; Zecchina, A.; Geobaldo, F.; Vlaic, G.; Bellatreccia, M. *J. Phys. Chem. B* **1997**, *101*, 344.

(33) Bolis, V.; Maggiorini, S.; Meda, L.; D'Acapito, F.; Palomino, G. T.; Bordiga, S.; Lamberti, C. *J. Chem. Phys.* **2000**, *113*, 9248.

(34) Zhang, Y. H.; Drake, I. J.; Bell, A. T. *Chem. Mater.* **2006**, *18*, 2347.

(35) Hoshino, Y.; Iwamoto, M. *Chem. Lett.* **1996**, 631.

(36) Kumashiro, P.; Kuroda, Y.; Nagao, M. *J. Phys. Chem. B* **1999**, *103*, 89.

(37) Bulanek, R. *Phys. Chem. Chem. Phys.* **2004**, *6*, 4208.

(38) Yamashita, H.; Matsuoka, M.; Tsuji, K.; Shioya, Y.; Anpo, M.; Che, M. *J. Phys. Chem.* **1996**, *100*, 397.

(39) Hadjiivanov, K. I.; Vayssilov, G. N. *Adv. Catal.* **2002**, *47*, 307.

(40) Davidova, M.; Nachtigallova, D.; Bulanek, R.; Nachtigall, P. *J. Phys. Chem. B* **2003**, *107*, 2327.

(41) Bulanek, R.; Cicmanec, P.; Knotek, P.; Nachtigallova, D.; Nachtigall, P. *Phys. Chem. Chem. Phys.* **2004**, *6*, 2003.

(42) Bludsky, O.; Nachtigall, P.; Cicmamec, P.; Knotek, P.; Bulanek, R. *Catal. Today* **2005**, *100*, 385.

(43) Zhang, Y. H.; Drake, I. J.; Briggs, D. N.; Bell, A. T. *J. Catal.* **2006**, *244*, 219.

(44) Nachtigallova, D.; Nachtigall, P.; Sierka, M.; Sauer, J. *Phys. Chem. Chem. Phys.* **1999**, *1*, 2019.

(45) *Accelrys, Materials Studio Getting Started*, Release 4.0; Accelrys Software, Inc.: San Diego, 2006.

(46) Sayle, D. C.; Catlow, C. R. A.; Gale, J. D.; Perrin, M. A.; Nortier, P. *J. Phys. Chem. A* **1997**, *101*, 3331.

(47) Balabanov, N. B.; Peterson, K. A. *J. Chem. Phys.* **2005**, *123*, 064107.

(48) Simon, S.; Duran, M.; Dannenberg, J. J. *J. Chem. Phys.* **1996**, *105*, 11024.

(49) Boys, S. F.; Bernardi, F. *Mol. Phys.* **1970**, *19*, 553.

(50) Meyer, F.; Chen, Y. M.; Armentrout, P. B. *J. Am. Chem. Soc.* **1995**, *117*, 4071.

(51) Nachtigallova, D.; Bludsky, O.; Arean, C. O.; Bulanek, R.; Nachtigall, P. *Phys. Chem. Chem. Phys.* **2006**, *8*, 4849.

(52) Bludsky, O.; Silhan, M.; Nachtigall, P.; Bucko, T.; Benco, L.; Hafner, J. *J. Phys. Chem. B* **2005**, *109*, 9631.

(53) Bludsky, O.; Silhan, M.; Nachtigallova, D.; Nachtigall, P. *J. Phys. Chem. A* **2003**, *107*, 10381.

(54) Feibelman, P. J.; Hammer, B.; Norskov, J. K.; Wagner, F.; Scheffler, M.; Stumpf, R.; Watwe, R.; Dumesic, J. *J. Phys. Chem. B* **2001**, *105*, 4018.

(55) Kresse, G.; Gil, A.; Sautet, P. *Phys. Rev. B* **2003**, *68*.

(56) Shao, L. M.; Zhang, L. N.; Zhou, M. F.; Qin, Q. Z. *Organometallics* **2001**, *20*, 1137.

(57) Rice, M. J.; Chakraborty, A. K.; Bell, A. T. *J. Catal.* **1999**, *186*, 222.

(58) Nachtigallova, D.; Nachtigall, P.; Sauer, J. *Phys. Chem. Chem. Phys.* **2001**, *3*, 1552.

(59) Schroder, K. P.; Sauer, J. C.; Leslie, M.; Richard, C.; Catlow, A. *Zeolites* **1992**, *12*, 20.

(60) Grau-Crespo, R.; Peralta, A. G.; Ruiz-Salvador, A. R.; Gomez, A.; Lopez-Cordero, R. *Phys. Chem. Chem. Phys.* **2000**, *2*, 5716.

(61) FEFF 8.0, http://feff.phys.washington.edu/.

(62) Ankudinov, A. L.; Ravel, B.; Rehr, J. J.; Conradson, S. D. *Phys. Rev. B* **1998**, *58*, 7565.

(63) Treesukol, P.; Limtrakul, J.; Truong, T. N. *J. Phys. Chem. B* **2001**, *105*, 2421.

(64) Kau, L. S.; Spirasolomon, D. J.; Pennerhahn, J. E.; Hodgson, K. O.; Solomon, E. I. *J. Am. Chem. Soc.* **1987**, *109*, 6433.